



HAL
open science

Preparation and properties of novel melt-blended halloysite nanotubes/wheat starch nanocomposites

Hélène Schmitt, Kalappa Prashantha, Jérémie Soulestin, Marie-France Lacrampe, Patricia Krawczak

► **To cite this version:**

Hélène Schmitt, Kalappa Prashantha, Jérémie Soulestin, Marie-France Lacrampe, Patricia Krawczak. Preparation and properties of novel melt-blended halloysite nanotubes/wheat starch nanocomposites. Carbohydrate Polymers, 2012, 89 (3), pp.920-927. 10.1016/j.carbpol.2012.04.037 . hal-01773163

HAL Id: hal-01773163

<https://hal.science/hal-01773163>

Submitted on 10 Apr 2024

HAL is a multi-disciplinary open access archive for the deposit and dissemination of scientific research documents, whether they are published or not. The documents may come from teaching and research institutions in France or abroad, or from public or private research centers.

L'archive ouverte pluridisciplinaire **HAL**, est destinée au dépôt et à la diffusion de documents scientifiques de niveau recherche, publiés ou non, émanant des établissements d'enseignement et de recherche français ou étrangers, des laboratoires publics ou privés.

Preparation and properties of novel melt-blended halloysite nanotubes/wheat starch nanocomposites

H. Schmitt^{a,b}, K. Prashantha^{a,b,*}, J. Soulestin^{a,b}, M.F. Lacrampe^{a,b}, P. Krawczak^{a,b}

^a Ecole des Mines de Douai, Department of Polymers and Composites Technology & Mechanical Engineering, 941 rue Charles Bourseul, BP 10838, F-59508 Douai, France

^b Univ. Lille Nord de France, Lille, F-59000, France

Novel bionanocomposites based on halloysite nanotubes as nanofillers and plasticized starch as polymeric matrix were successfully prepared by melt-extrusion for the first time. Both modified and non modified halloysites were added at different weight contents. The structural, morphological, thermal and mechanical properties of plasticized starch/halloysites nanocomposites were investigated. Melt-compounding appears to be a suitable process to uniformly disperse nanotubes in the plasticized starch matrix. Interactions between plasticized starch and halloysites in the nanocomposites and microstructure modifications were monitored using Fourier transfer infrared spectroscopy, X-ray diffraction and dynamic mechanical analysis. Addition of halloysite nanotubes slightly enhances the thermal stability of starch (onset temperature of degradation delayed to higher temperatures). The tensile mechanical properties of starch are also significantly improved (up to +144% for Young's modulus and up to +29% for strength) upon addition of both modified and unmodified halloysites, interestingly without loss of ductility. Modified halloysites lead to significantly higher Young's modulus than unmodified halloysites.

1. Introduction

In recent years, the development of new biopolymers obtained from renewable resources has been driven by the necessity to limit the carbon footprint of polymeric materials. In this context, the usage of starch in non-food applications is known to be of an unprecedented interest. Starch is a complex polysaccharide mainly composed of linear amylose and non-linear amylopectin. The amylose and amylopectin represent approximately 98–99% of the dry weight. The ratio of the two polysaccharides varies according to the botanical origin of the starch. The waxy starch contains less than 1% amylose, normal starch contains 18–33% of amylose and high amylose starch contains as much as 70% of amylose (Buléon, Colonna, Planchota, & Ballb, 1998). The moisture content air-equilibrated starch ranges from about 10–12% (starch from the cereal) to about 14–18% (starch from some roots and tubers) (Tester, Karkalasa, & Qi, 2004). Amylose is defined as a linear chain of (1→4)- α -linkages to D-glucose with some molecules slightly branched by (1→6)- α -linkages. Amylopectin is composed of short-chain molecule, forming a tree. Its structure is highly branched, built of about 95% of (1→4)- α -linkage and 5% (1→6)- α -linkages. The association of amylose and amylopectin, in the native state, gives a semi-

crystalline structure (15–45%). The crystallinity of native starch can be observed using polarized light microscopy when a Maltese cross is seen. Depending on the botanical origin of starch, different structures are distinguished by X-ray diffraction namely A, B and C-type crystalline structures (Van Soest, Benes, & De Wit, 1996).

Unfortunately, native starch is brittle and its mechanical properties are very poor (Freire, Podczeczek, Veiga, & Sousa, 2009; García, Famá, Dufresne, Aranguren, & Goyanes, 2009). In the absence of water, thermal degradation occurs below the glass transition temperature (Chivrac, Pollet, & Avérous, 2009). Therefore, native starch must be plasticized before processing and moulding. After plasticization, three different crystal structures (namely V_A-, V_H- and E_H-types) can be observed depending on processing (Van Soest, Hulleman, De Wit, & Vliegthart, 1996). The manufacturing of starch-based polymers then becomes economically viable and can be achieved using traditional plastics processing technologies such as extrusion, injection-moulding, compression and film casting (Liu, Xie, Yu, Chen, & Li, 2009; Mondragón, Hernández, Rivera-Armenta, & Rodríguez-González, 2009; Xie, Chang, Wang, Yu, & Ma, 2011). The continuous and cost effective hot melt-extrusion process is however usually preferred, because of greater disruption of starch structure (Yu & Christie, 2001). Nevertheless, due to its poor mechanical properties and moisture sensitivity, plasticized starch cannot compete with petroleum based polymers yet. To overcome these issues, plasticized starch can be reinforced by fillers, leading to the formation of a composite material (Chung et al., 2010; Soulestin, Prashantha, Lacrampe, & Krawczak, 2011). A new class of

* Corresponding author at: Ecole des Mines de Douai, Department of Polymers and Composites Technology & Mechanical Engineering, 941 rue Charles Bourseul, BP 10838, F-59508 Douai, France. Tel.: +33 327712169; fax: +33 327712981.

E-mail address: kalappa.prashantha@mines-douai.fr (K. Prashantha).

composite materials, namely nanocomposites, based on nano-sized fillers such as carbon nanotubes and nanoclay (especially montmorillonite) has been recently investigated. Due to high aspect ratio and geometry of these nanofillers, drastic modifications may be expected in plasticized starch (Chivrac et al., 2009; Soulestin et al., 2011).

Halloysite nanotubes have recently become the subject of research attention as a new type of a nanofiller for enhancing the mechanical (Ismail, Pasbakhsh, Fauzi, & Abu Bakar, 2008; Prashantha, Lacrampe, & Krawczak, 2011; Prashantha, Schmitt, Lacrampe, & Krawczak, 2011), thermal (Ismail et al., 2008; Xie et al., 2011) and fire retardant (Marney, Ruisell, & Wu, 2008) performance, and the degree of crystallinity (Prashantha, Schmitt, et al., 2011; Szczygielska & Kijenski, 2011; Xie et al., 2011) of thermoplastic polymers. Halloysite is an aluminosilicate, chemically similar to kaolin, mined from natural deposits and formed from amorphous allophane by long time weathering (Levis & Deasy, 2002). According to their origin, halloysites can be found in different forms such as short tubes, large tubes and spheroids (Joussein et al., 2005). Common halloysites used for polymer reinforcement are in form of fine, tubular structures of 300–1500 nm length, 15–100 nm inner diameter and 40–120 nm outer diameter (Du, Guo, & Jia, 2010). Halloysites are made of layers separated by a monolayer of water molecules. X-ray diffraction allows two forms of halloysites to be distinguished. Hydrated and dehydrated halloysites have a basal (d_{001}) spacing of 10 Å and 7 Å, respectively. The chemical formula of halloysite is $\text{Al}_2\text{Si}_2\text{O}_5(\text{OH})_4 \cdot n(\text{H}_2\text{O})$ with n equal to 0 and 2 for hydrated and dehydrated halloysites, respectively. A partially hydrated form can be observed; in this case, a diffuse peak appears between 7 Å and 10 Å (Levis & Deasy, 2002). As the inter-layer water is weakly attached, hydrated halloysite can be irreversibly transformed into the dehydrated form by simple heating at a temperature below 110 °C. Halloysite layers can be represented by a superposition of a sheet of gibbsite (octahedral of alumina bonded to hydroxyl groups) and a siloxane sheet (tetrahedral of silica bonded to oxygen ions) (Nicolini, Fukamachi, Wypych, & Mangrich, 2009). Tubes are formed by the rolling of two layered aluminosilicate kaolin due to the strain caused by lattice mismatch between the adjacent sheets of silicon dioxide and aluminium oxide (Hope & Kittrick, 1964). Therefore, there are two types of hydroxyl groups, internal groups being located between the layers and external groups being located on the surface. Compared with others silicates such as kaolinite and montmorillonite, the density of surface hydroxyl groups of halloysites is much smaller. Therefore by the combination between a high aspect ratio and a low density of surface hydroxyl group, halloysites nanotubes are very promising as reinforcing fillers for polymer materials (Du et al., 2010).

Recently, plasticized starch/halloysite nanocomposites were prepared by solvent casting (He et al., 2012; Xie et al., 2011), which is not very practical in polymer processing industries. Melt-extrusion would be more productive and efficient in industrial workshops. However, to the best of our knowledge, detailed investigations on the melt-compounding and the characterization of plasticized starch/halloysites nanocomposites have not been reported in the literature yet. Therefore, the present study aims at developing plasticized starch/halloysites nanocomposite prepared by direct melt-blending. The structural and mechanical properties of the obtained nanocomposites will be assessed as a function of the halloysites content and surface treatment.

2. Experimental

2.1. Materials

Wheat starch (Roquette, France) was used in this study. In order to limit fluctuations in water content, it was stored at 23 °C

with 50% relative humidity (RH). In these conditions, the native starch contains 12% of the original moisture. The non-volatile plasticizer was glycerol (99% purity) (Sigma–Aldrich, France). The lubricant was glycerol monostearate (Mosselman, Belgium). The fillers were unmodified halloysites nanotubes (HNT) and quaternary ammonium salt with benzoalkonium chloride treated halloysite nanotubes (MHNT) (Natural Nano Inc., USA). The halloysites used have a density of 2.5 g/cm³ and a tubular structure with 100–120 nm outer diameter, 60–80 nm inner diameter and lengths typically ranging from about 500 nm to over 1.2 μm. Before processing, fillers were dried in an oven at 80 °C for 12 h in order to eliminate moisture.

2.2. Preparation of nanocomposites

Plasticized starch/halloysites nanocomposites were produced in two steps. At first, 75 wt% native starch, 24 wt% glycerol, 1 wt% glycerol monostearate and required amount of halloysites were physically blended in a mechanical mixer for 3 h at room temperature. Then, these mixtures were processed in a twin-screw extruder (Haake Rheomex PTW 16 OS, Thermo Scientific, Germany) at a screw speed of 60 rpm. The screw diameter was 16 mm and the screw ratio L/D 40. The temperature setting from the hopper to the die was 110–115–120 °C. Nanocomposites containing 2, 4, 6 and 8 wt% nanotubes were compounded (designated as GSx% for HNTs and GSMx% for MHNTs, x taking the value 2, 4, 6 or 8 accordingly).

After pelletizing and conditioning at 23 °C and 50% HR during 24 h, all materials were injection-moulded (Babyplast 6/10P, Cronoplast, Italy) into a standard test specimen for tensile and dynamic mechanical analysis. The typical injection-moulding conditions were the following: temperature profile setting from 145 to 150 °C, flow rate of 1.3 cm³ s⁻¹, holding pressure of 50 bars, and cooling time of 10 s.

Before testing, all samples were stored in controlled humidity chamber for four weeks at 23 °C with a controlled relative humidity (HR) of 53% using saturated solution of magnesium nitrate. The moisture content of all the samples was determined using a Karl Fischer titrator (V30, Mettler-Toledo, France) combined with an oven (Mettler Stromboli, France). It was found to be 9.5 ± 0.4 wt%.

2.3. Characterization

The fracture surfaces of the materials were observed by scanning electron microscopy (SEM) under high vacuum with a SEM instrument (S-4300SE/N, Hitachi, Japan) operating at 5 kV, the injection-molded cryofractured samples being previously coated with a thin gold layer.

The chemical structure of the materials was analyzed by Fourier transform infrared (FTIR) spectroscopy (Nicolet 380 FT-IR, Thermo Scientific, France). For this purpose, the native starch and halloysites powders (1 mg) were mixed with KBr (4 mg) and then formed into a disc in a manual press at room temperature. Transmission spectra of nanocomposites were recorded using a microscope in transmission mode on 5 μm thick sample slices cut with a microtome (Leica RM2165, Switzerland). Transmission spectra were recorded using at least 32 scans with 4 cm⁻¹ resolution, in the spectral range 4000–600 cm⁻¹.

The X-ray diffraction patterns of the materials were recorded using an X-ray diffractometer (D8 Advance, Bruker, Germany). The data collection was performed with a Co K_α cathode and a detector (Lynxeye, Bruker, Germany). The monochromator was used at a voltage of 40 kV and an intensity of 40 mA. The scattering angles (2θ) range from 5° to 40° at an interval of 0.02°. The height of the peaks was measured from baseline and the baseline passed through the lowest point of the diffractogram, which is parallel to the x -axis.

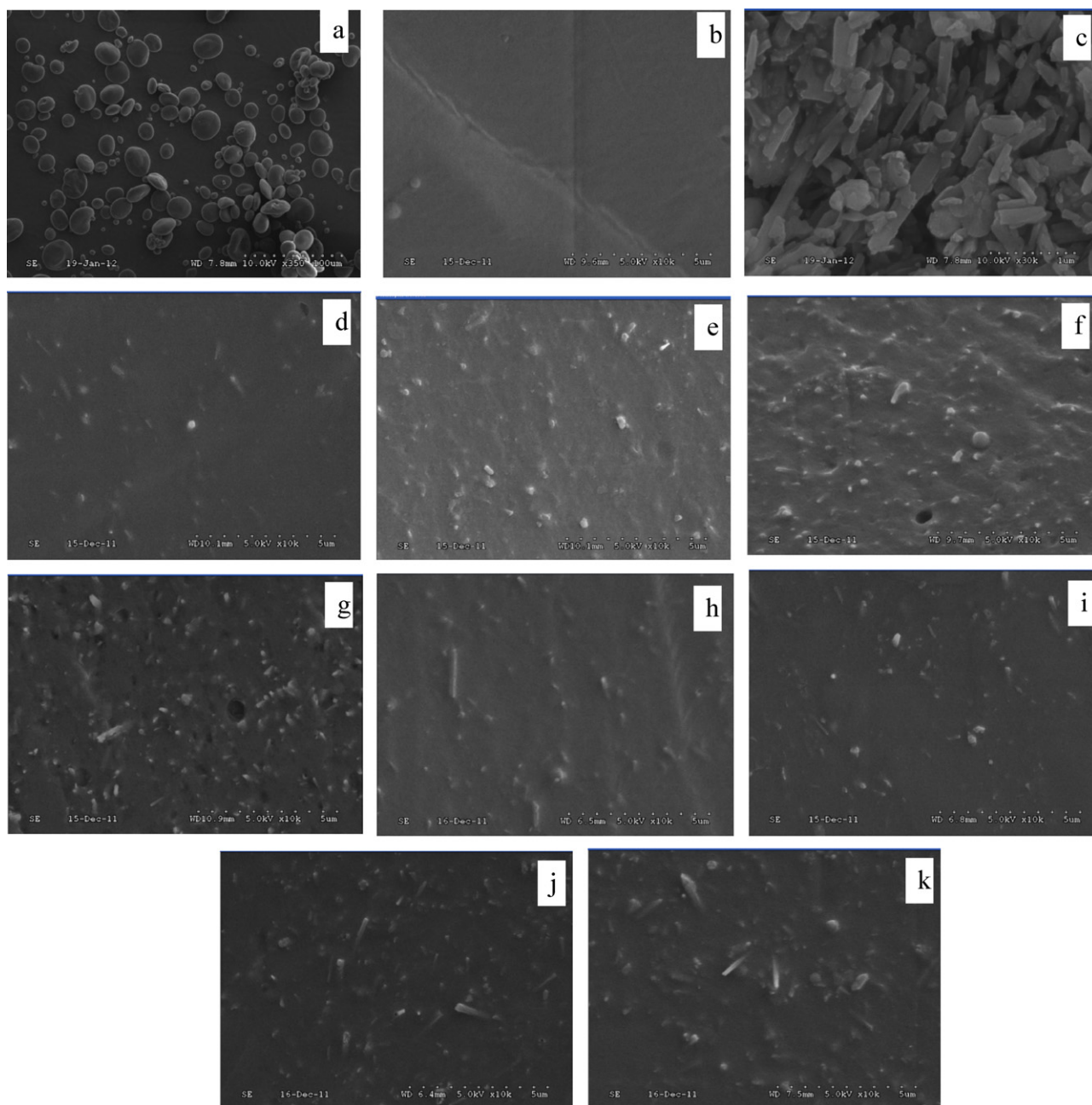


Fig. 1. SEM images of native starch (a), plasticized starch (b), halloysites (c), plasticized starch/unmodified halloysite nanocomposites: 2 wt% HNT (d), 4 wt% HNT (e), 6 wt% HNT (f), 8 wt% HNT (g) and plasticized starch/modified halloysite nanocomposites: 2 wt% MHNT (h), 4 wt% MHNT (i), 6 wt% MHNT (j), 8 wt% MHNT (k).

The thermal stability of the samples was measured with a thermogravimetric analyser (TGA, Mettler, France). Sample masses ranging from 3 and 5 mg were heated from 25 °C to 600 °C at a rate 20 °C min⁻¹ in a dry nitrogen atmosphere. The flow rate of nitrogen was 20 ml min⁻¹.

The viscoelastic behaviour was studied in tension by dynamic mechanical analysis (DMA+150, Metravib, France) at a frequency of 10 Hz. The displacement amplitude was 3.5 µm. Data were collected from -80 °C to 100 °C at a scanning rate of 2 °C min⁻¹. DMA specimens (4 mm × 10 mm × 15 mm) were cut from injection-moulded impact bar samples. Three specimens of each composition were tested at least.

The mechanical properties were evaluated from injection-moulded specimens. Tensile properties were measured using a tensile machine (Model 1185 Instron, USA) equipped with a 1 kN force sensor at a crosshead speed of 10 mm min⁻¹ at 23 °C and 50%

RH according to the ISO 527 standard. At least five specimens of each composition were tested.

3. Results and discussion

3.1. Nanotube dispersion

SEM images of native starch, plasticized starch and halloysites are illustrated in Fig. 1. The granular characteristic of native starch (Fig. 1a) is no longer visible in the plasticized starch (Fig. 1b) attesting the high ratio of destructuration of the native starch after plasticization by melt-extrusion process. SEM images of the nanocomposites show that both modified and unmodified halloysites are uniformly dispersed in the plasticized starch matrix (Fig. 1d-k). Homogenous dispersion of halloysites with a majority of individual nanotubes is observed up to 6 wt% of HNT or MHNT.

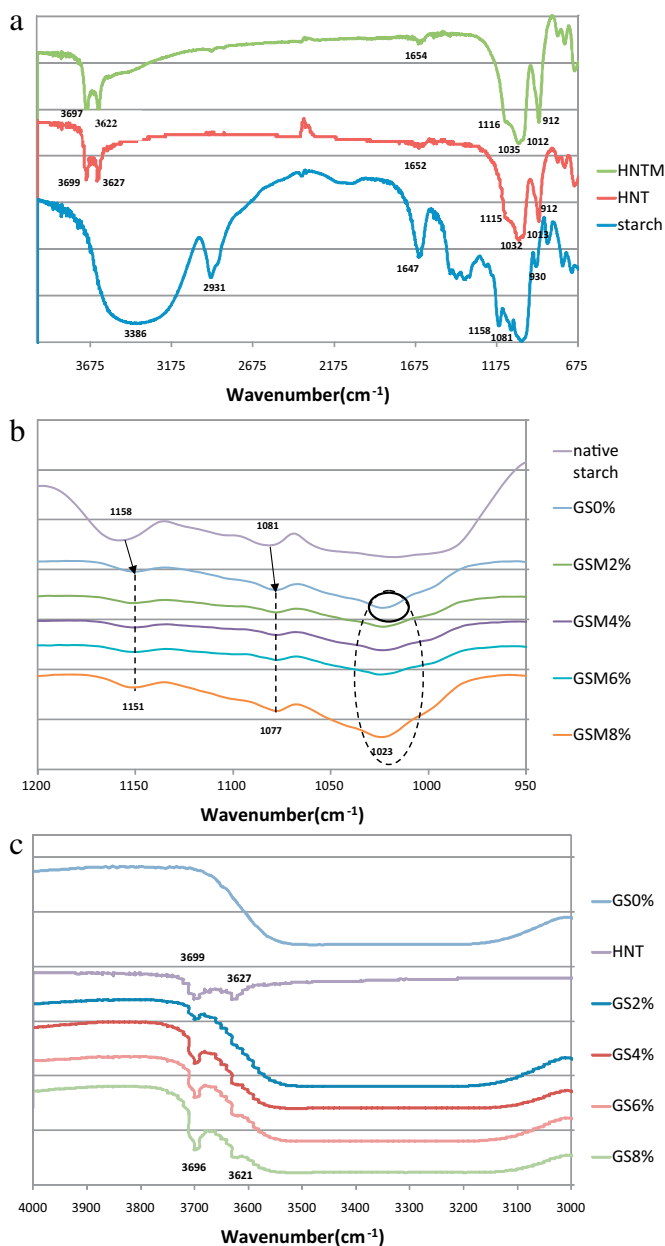


Fig. 2. (a) FTIR spectra of unmodified (HNT), modified (MHNT) halloysites, native starch. (b) FTIR spectra of native starch, plasticized starch and starch/halloysites nanocomposites at different modified halloysites (MHNT) contents. (c) FTIR spectra of native starch, plasticized starch and starch/halloysites nanocomposites at different unmodified halloysites (HNT) contents.

Aggregates are visible at higher loading (8 wt%) of HNT or MHNT (Fig. 1g and k, respectively). Besides, the interface between MHNTs and plasticized starch matrix seems to be very good without any sign of debonding (Fig. 1j and k). In comparison, the presence of voids or holes (Fig. 1f and g) suggests that the interface between unmodified halloysites and plasticized starch is of poorer quality.

3.2. Chemical interactions

Interactions between plasticized starch and halloysites in the nanocomposites were verified using Fourier transfer infrared spectroscopy. The characteristic peaks of native starch and neat halloysites were determined (Fig. 2a). Their assignment is reported Table 1. Similarly, the FTIR spectra of plasticized starch and

starch/halloysites nanocomposites (Fig. 2b and c) were also recorded.

During the plasticization process, plasticizers and water added into native starch played a key role, by forming hydrogen bonding with starch in order to make plasticized starch (Hulleman, Janssen, & Feii, 1998). The position of neat plasticized starch (GS0%) peaks shifts to lower wave numbers (1151 and 1077 cm⁻¹) compared to that of native starch peaks (1158 and 1081 cm⁻¹), and a new peak at 1023 cm⁻¹ appears (Fig. 2b). This modification indicates the creation of stable hydrogen bonds between the starch and the plasticizer (Ma, Yu, & Wan, 2006). The same trend was observed for plasticized starch reinforced with modified halloysites (GSM2–8%, Fig. 2b), and with unmodified halloysites (GS2–8%, not represented in the Fig. 2b).

In the nanocomposites with unmodified fillers, the peaks of halloysites corresponding to the internal and external hydroxyl groups (3699 and 3627 cm⁻¹ for neat HNTs) weakly shift to lower wave numbers (3696 and 3621 cm⁻¹ respectively for GS2–GS8) (Fig. 2c). This may be explained by the formation of the interactions between external hydroxyl groups of halloysites and C–O–C groups of starch (Nicolini et al., 2009) and/or glycerol. The same trend is observed for the nanocomposites containing modified halloysites (not represented in the Fig. 2c).

3.3. Microstructure

The changes in the microstructure of plasticized starch upon addition of HNT or MHNT were studied by XRD (Fig. 3). XRD was also used to verify the dehydrated form of halloysites. The diffractograms of modified and unmodified halloysites show characteristic peaks at 7.41 Å ($2\theta_{Co} = 13.90^\circ$), 4.52 Å ($2\theta_{Co} = 23.19^\circ$) and 3.74 Å ($2\theta_{Co} = 28.42^\circ$) corresponding to basal spacings of d_{001} , d_{020} and d_{002} respectively. The absence of peak at 10 Å confirms the dehydrated form of halloysites due to drying before processing (Levis & Deasy, 2002).

The diffractogram of native starch shows peaks at 5.83 ($2\theta_{Co} = 17.78^\circ$), 5.18 ($2\theta_{Co} = 20.10^\circ$), 4.92 ($2\theta_{Co} = 21.21^\circ$), 4.48 ($2\theta_{Co} = 23.41^\circ$) and 3.90 Å ($2\theta_{Co} = 27.16^\circ$) characteristic of the A-type crystal of the cereal starch (Buléon et al., 1998; Hulleman et al., 1998).

Plasticization of native starch (GS0%) induces the transformation of the A-type crystalline structure to the B-type and V_H-type structures characterized by the appearance of peaks located at 4.85 ($2\theta_{Co} = 21.53^\circ$), 4.29 Å ($2\theta_{Co} = 24.51^\circ$) and 6.76 ($2\theta_{Co} = 15.27^\circ$), 4.51 ($2\theta_{Co} = 23.26^\circ$), 4.03 Å ($2\theta_{Co} = 26.21^\circ$) respectively. This mixed structure (B- and V_H-types) is known to be promoted by low extrusion water content and high extrusion temperature (Forsella, Mikkilä, Moates, & Parker, 1997) wherein V_H-type being characteristic of a better plasticization.

The halloysites characteristic peaks at 7.41 Å ($2\theta_{Co} = 13.80^\circ$) and 3.74 Å ($2\theta_{Co} = 28.42^\circ$) remain visible in the diffractogram of the nanocomposites (for both HNT and MHNT). The height of their peaks apparently increases with increase in halloysites content (Table 2). The plasticized starch peaks are also present in the diffractogram of the nanocomposites. These results confirm that halloysites nanotubes are dispersed in the starch matrix (Carli, Crespo, & Mauler, 2011).

The type of the halloysites (HNT or MHNT) influences the crystalline structure of the plasticized starch matrix. The addition of MHNT at the lowest content (2 wt%) reduces the formation of the V_H-type structure of the plasticized starch and favours the formation of B-type structure. This means that addition of a low content of MHNT reduces the starch plasticization (so-called plasticization reverse effect). Further addition of MHNT induces an increase of the height of V_H-type structure peaks which regain the initial height (GS0%) at about 8 wt% of MHNT (Table 2). The reverse effect

Table 1
FTIR assignments for native starch and halloysites.

	Peaks (cm ⁻¹)	Assignment
Native starch	3600–3900	—OH bond
	2931	—C—H and —C—H ₂ bond stretching of the anhydroglucose ring
	1647	Water bonding vibration
	1160–1080	—C—O bond stretching of the —C—O—H bonds
	1039–990	—C—O bond stretching of the C—O—C group in the anhydroglucose ring
Halloysite	3700–3600	External hydroxyl group and internal hydroxyl groups
	1650	Water deformation bond
	1200–1000	—Si—O bond vibration and stretching
	912	—O—H deformation of the inner hydroxyl group

Table 2
Evolution of the position, height of the halloysites XRD characteristic peaks (7.41 Å and 3.74 Å) in plasticized starch/halloysites nanocomposites and height of the XRD characteristic peaks of the starch type-B and type-V_H crystalline structure.

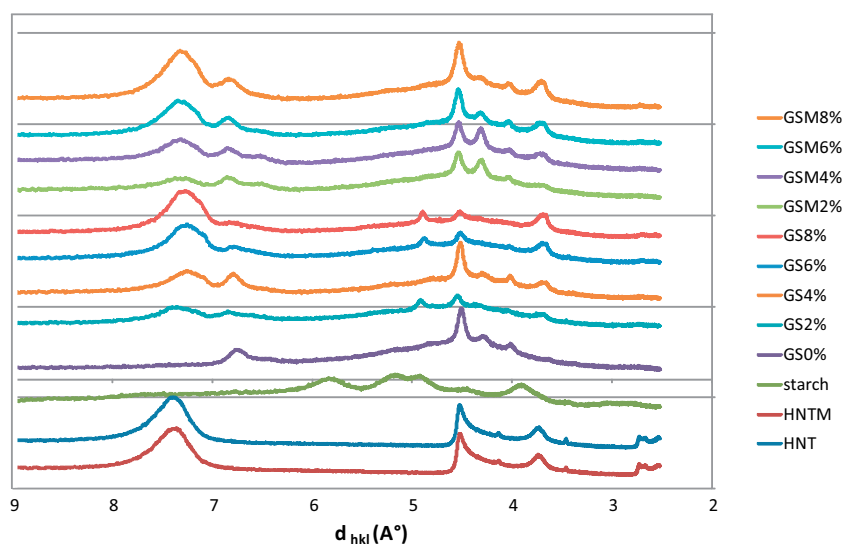
		Halloysite peak at 7.41 Å		Halloysite peak at 3.74 Å		B-type structure		V _H -type structure		
		Peak (Å)	Height	Peak (Å)	Height	Height of the peak at 4.85 Å	Height of the peak at 4.29 Å	Height of the peak at 6.76 Å	Height of the peak at 4.51 Å	Height of the peak at 4.03 Å
Plasticized starch	GS0%					0.99	3.13	5.86	17.25	3.60
HNT-based nanocomposites	GS2%	7.39	5.86	3.68	2.39	4.28	–	2.38	5.48	1.05
	GS4%	7.25	7.95	3.65	3.58	0.52	1.93	6.43	18.52	3.12
	GS6%	7.18	7.95	3.63	6.11	1.74	0.54	2.19	8.27	1.58
	GS8%	7.26	18.02	3.66	7.70	5.74	–	1.05	4.03	0.30
MHNT-based nanocomposites	GSM2%	7.32	4.46	3.69	1.70	–	7.54	4.20	11.65	2.45
	GSM4%	7.32	8.53	3.70	3.87	–	9.55	4.35	12.47	2.22
	GSM6%	7.31	13.45	3.70	5.89	–	3.49	5.68	15.77	2.83
	GSM8%	7.31	20.41	3.70	8.43	–	2.89	6.04	20.85	3.80

on the starch plasticization induced by the addition of the lowest halloysites content is more pronounced for HNT than for MHNT. Further increase in HNT content does not allow compensation of the initial reverse effect due to HNT addition (except for 4 wt% surprisingly). This may be due to the interactions between HNT and glycerol; therefore the availability of glycerol for plasticization is less. On the opposite, because of their surface treatment, the affinity of modified halloysites with glycerol was lower and glycerol was completely available for plasticization (Shi et al., 2007).

3.4. Thermal behaviour (TGA).

For plasticized starch (GS0%), the mass loss curves falls in three steps, the first above 100 °C, the second above 250 °C and the third at 331 °C. The first mass loss is mainly related to the water volatilization, the second one to the plasticizer volatilization. The significant mass loss at the highest temperature may be ascribed to the decomposition of starch.

The first two steps are not affected by the addition of the halloysites (HNT or MHNT). On the contrary, the onset temperature of

**Fig. 3.** XRD patterns of unmodified (HNT) or modified (MHNT) halloysites, native starch, plasticized starch and plasticized starch/halloysites nanocomposites at different halloysites contents.

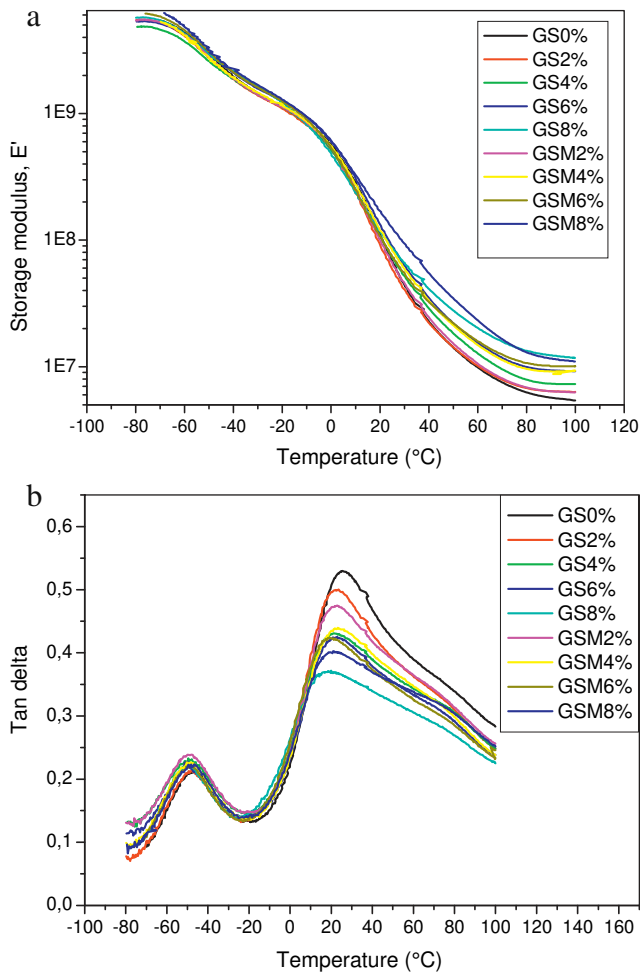


Fig. 4. $\tan\delta$ (a) and storage modulus (E') (b) vs temperature for plasticized starch and plasticized starch/HNTs and plasticized starch/MHNTs nanocomposites at different halloysites contents.

starch decomposition is delayed to higher temperatures in case of nanocomposites, and this transition increases with increasing halloysites content (331, 335, 337, 338 respectively for GS2%–GS8% and 336, 336, 337, 338 respectively for GSM2%–GSM8%). Thus, the addition of halloysites increases the thermal stability of the matrix. This may be explained by the high thermal stability of halloysites and interaction between plasticized starch and halloysites (Xie et al., 2011).

3.5. Viscoelastic behaviour

Dynamic mechanical analysis (DMA) was carried out to get more information about molecular motion and structure with a focus on interfacial interaction between the nanocomposites components. It is also an effective tool to study the strain response of polymers exposed to dynamic forces.

For plasticized starch (GS0%), the loss factor ($\tan\delta$) shows two peaks at -47°C and 25°C (Fig. 4a). The $\tan\delta$ peak is commonly referred to relaxations of the polymer related to glass transition temperature (T_g) or secondary transitions. The position of the upper transition is commonly associated to the glass transition of the starch rich phase (T_α) while the lower one is attributed to the glass transition of the glycerol rich phase (T_β) (Forssella et al., 1997). The variation in $\tan\delta$ of the nanocomposite is similar to that of plasticized starch. Nevertheless, the transition corresponding to the plasticizer rich phase (-47°C) remains identical for all

Table 3

Tensile properties of plasticized starch and plasticized starch/halloysites nanocomposites.

		Young's modulus (MPa)	Tensile strength (MPa)	Elongation at break (%)	
Plasticized starch	GS0%	12.82 ± 2.35	2.28 ± 0.08	87 ± 5	
	HNT-based nanocomposites	GS2%	13.96 ± 1.92	2.42 ± 0.12	85 ± 1
		GS4%	18.56 ± 0.54	2.82 ± 0.03	85 ± 3
		GS6%	20.83 ± 1.96	2.81 ± 0.10	84 ± 2
GS8%		25.01 ± 3.33	2.93 ± 0.16	83 ± 4	
MHNT-based nanocomposites	GSM2%	16.53 ± 5.58	2.72 ± 0.14	87 ± 4	
	GSM4%	19.06 ± 1.06	2.79 ± 0.04	82 ± 3	
	GSM6%	21.74 ± 5.72	2.81 ± 0.15	89 ± 5	
	GSM8%	31.33 ± 2.65	2.93 ± 0.34	83 ± 7	

the materials whereas the transition corresponding to the starch rich phase (25°C) is shifted to the lower temperature in presence of HNT. The amplitude of this shift decreases with increasing halloysites content. Moreover the height of peak decreases with increasing halloysites content, which may indicate a restriction of the motion of polymer chains and an effective interfacial interaction between the halloysites and the starch matrix (Lu & Nutt, 2003). The same results are obtained upon MHNT addition (Fig. 4a).

The storage modulus (E') of all HNT-based nanocomposites (GS2–8%) is higher than that of neat plasticized starch (GS0%) and increases with increasing halloysites content (Fig. 4b). This is caused by the restrictions of the segmented motion of the starch chains (Zhou et al., 2009) and the presence of nanotubes with high modulus and high aspect ratio (Guimaraes, Enyashin, Seifert, & Duarte, 2010). This trend is mainly visible above of the glass transition of the starch rich phase (T_α). The same results are obtained for MHNT-based nanocomposites (Fig. 4b).

3.6. Mechanical behaviour

Tensile stress–strain curves of plasticized starch/HNT and plasticized starch/MHNT nanocomposites were recorded (Fig. 5a). Stress increases continuously with strain without yielding until fracture; considering the high elongation at break, the behaviour is typically plastic. The deformation mechanism of the plasticized starch does not change upon addition of the nanofiller. The tensile properties of starch/HNT and starch/MHNT nanocomposites containing different halloysites weight contents were computed (Table 3 and Fig. 5b and c). Tensile modulus (E), tensile strength (σ_R) and elongation at break (ε_R) of plasticized starch are equal to 12.82 MPa, 2.28 MPa and 87%, respectively. The addition of both unmodified and modified halloysites significantly increases the Young's modulus and the tensile strength without any loss of ductility.

In case of plasticized starch/HNT nanocomposites, tensile strength and elastic modulus increase up to 28% and 95%, respectively. In the case of plasticized starch/MHNT nanocomposites, tensile strength and elastic modulus increase up to 29% and 144%, respectively. This result is consistent with previous DMA results and morphology analysis. The enhancement of mechanical properties upon halloysites addition is due to high aspect ratio and high mechanical properties of halloysites combined to good compatibility between starch and such filler (Yang, Shi, Pramoda, & Goh, 2007). Indeed, good interfacial adhesion between halloysites and starch along with homogeneous dispersion of halloysites in starch matrix enables efficient stress transfer from the matrix to reinforcements, which gives rise to tensile strength. Moreover, modified halloysites (MHNT) lead to better mechanical properties (compared to unmodified HNT). This is in accordance with SEM observations, where no debonded MHNTs are observed due to the improved interface between MHNTs and starch matrix (compared with that between HNTs and starch matrix). Such an increase in strength and modulus

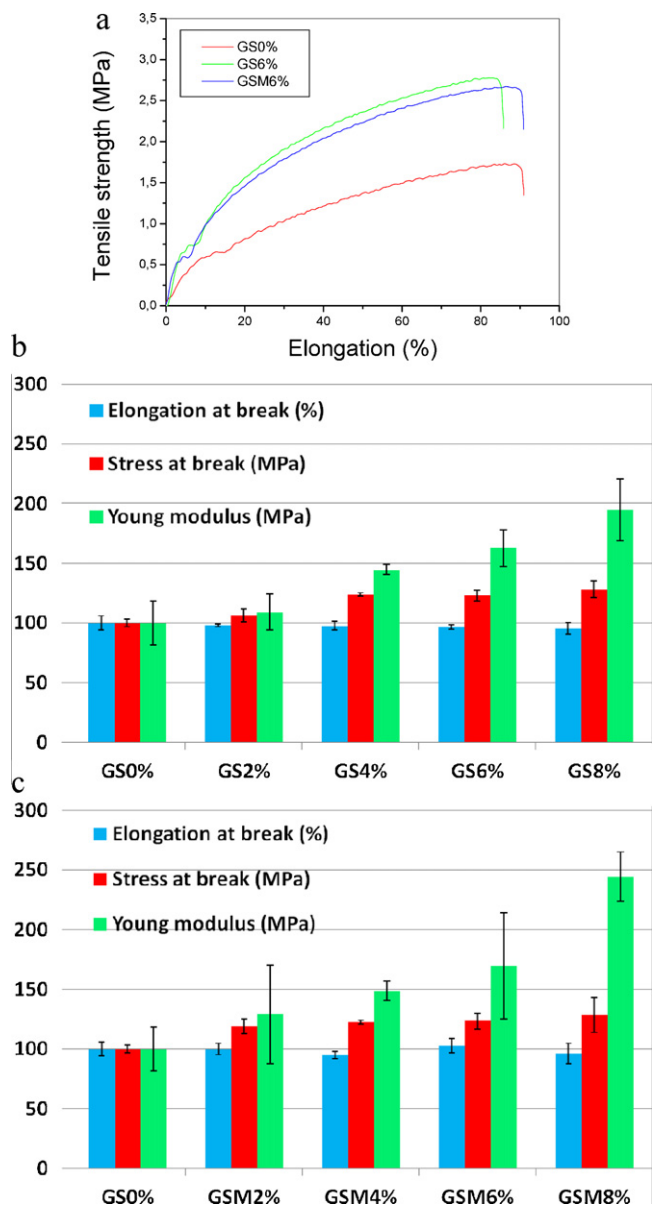


Fig. 5. (a) Typical tensile stress–strain curves of plasticized starch and plasticized starch bearing 6 wt% halloysites content. (b) Tensile properties of plasticized starch and plasticized starch/HNT nanocomposites at different halloysites contents. (c) Tensile properties of plasticized starch and plasticized starch/MHNT nanocomposites at different halloysites contents.

may be partly related to the material crystalline structure variations. The modulus increase may be related to an initial increase in the formation of double helical structures of the amylopectin (Van Soest, De Wit, & Vliegthart, 1996) which reduces the mobility of the amylopectin molecules. The strength increase may be explained by the reduction in the plastic flow of crystalline materials, and also due by the rupture of covalent bonds (Van Soest, De Wit, et al., 1996). However the improvement of the mechanical behaviour in tension is mainly ascribed to the homogeneous dispersion of halloysites in starch matrix.

4. Conclusion

Plasticized starch/halloysite nanotubes nanocomposites were prepared by melt-extrusion process in a twin-screw extruder. The efficiency of melt-compounding in dispersing the nanotubes in

starch matrix was evidenced by scanning electron microscopy. The influence of halloysite content and their modification on the structural and mechanical properties of the nanocomposites were investigated. Interactions between plasticized starch and halloysites in the nanocomposites and microstructure modifications were monitored using Fourier transfer infrared spectroscopy, X-ray diffraction and dynamic mechanical analysis. The thermal stability and mechanical properties of starch are significantly improved upon addition of both modified and unmodified halloysites into starch matrix. Modified halloysites leading to significantly higher Young's modulus than unmodified halloysites. Compared to other nanofillers used to improve mechanical properties of plasticized starch prepared by melt-extrusion, the addition of halloysites nanotubes allows achieving better combination of properties (thermal stability, tensile modulus, strength and elongation at break).

Wheat starch is a cheap raw material, abundant, renewable, readily available and very versatile in terms of chemical and physical modification, whilst halloysite is natural and biocompatible. Thus, fully bio-based plastic materials with improved mechanical properties are achievable by adequately adjusting the composition of the nanocomposite system. Further assessment of this nanocomposite system for biomedical application is in progress in our group.

Acknowledgments

Authors would like to thank International Campus on Safety and Intermodality in Transportation (CISIT), Nord-Pas-de-Calais Region and European Community (FEDER).

References

- Buléon, A., Colonna, P., Planchota, V., & Ballb, S. (1998). Starch granules: Structure and biosynthesis. *International Journal of Biological Macromolecules*, 23, 85–112.
- Carli, L. N., Crespo, J. S., & Mauler, R. S. (2011). PHBV nanocomposites based on organomodified montmorillonite and halloysite: The effect of clay type on the morphology and thermal and mechanical properties. *Composites Part A: Applied Science and Manufacturing*, 42, 1601–1608.
- Chivrac, F., Pollet, E., & Avérous, L. (2009). Progress in nano-biocomposites based on polysaccharides and nanoclays. *Materials Science and Engineering R: Reports*, 67, 1–17.
- Chung, L., Ansari, S., Estevez, L., Hayrapetyan, S., Giannelis, E. P., & Lai, H. M. (2010). Preparation and properties of biodegradable starch–clay nanocomposites. *Carbohydrate Polymers*, 79, 391–396.
- Du, M., Guo, B., & Jia, D. (2010). Newly emerging applications of halloysite nanotubes: A review. *Polymer International*, 59, 574–582.
- Forcella, P. M., Mikkilä, J. M., Moates, G. K., & Parker, R. (1997). Phase and glass transition behaviour, of concentrated barley starch–glycerol–water mixtures, a model for thermoplastic starch. *Carbohydrate Polymers*, 34, 275–282.
- Freire, C., Podczcek, F., Veiga, F., & Sousa, J. (2009). Starch-based coatings for colon-specific delivery. Part II. Physicochemical properties and in vitro drug release from high amylose maize starch films. *European Journal of Pharmaceutics and Biopharmaceutics*, 72, 587–594.
- García, N. L., Famá, L., Dufresne, A., Aranguren, M., & Goyanes, S. (2009). A comparison between the physico-chemical properties of tuber and cereal starches. *Food Research International*, 42, 976–982.
- Guimaraes, L., Enyashin, A. N., Seifert, G., & Duarte, H. A. (2010). Structural, electronic, and mechanical properties of single-walled halloysite nanotube models. *Journal of Physical Chemistry C*, 114, 11358–11363.
- He, Y., Kong, W., Wang, W., Liu, T., Liu, Y., Gong, Q., et al. (2012). Modified natural halloysite/potato starch composite films. *Carbohydrate Polymers*, 87, 2706–2711.
- Hope, E. W., & Kittick, J. A. (1964). Surface tension and the morphology of halloysites. *The American Mineralogist*, 49, 859–866.
- Hulleman, S. H. D., Janssen, F. H. P., & Feij, H. (1998). The role of water during plasticization of native starches. *Polymer*, 39, 2043–2048.
- Ismail, H., Pasbakhsh, P., Fauzi, M. N. A., & Abu Bakar, A. (2008). Morphological, thermal, and tensile properties of halloysites nanotubes filled ethylene propylene diene monomer (EPDM) nanocomposites. *Polymer Testing*, 27, 841–850.
- Joussein, E., Petit, S., Churuchman, J., Theng, B., Righi, D., & Delvaux, B. (2005). Halloysite clays mineral—A review. *Clay Mineral*, 40, 383–426.
- Levis, S. R., & Deasy, P. B. (2002). Characterisation of halloysite for use as a microtubular drug delivery system. *International Journal of Pharmaceutics*, 243, 125–134.
- Liu, H., Xie, F., Yu, L., Chen, L., & Li, L. (2009). Thermal processing of starch-based polymers. *Progress in Polymer Science*, 34, 1348–1368.
- Lu, H. B., & Nutt, S. (2003). Restricted relaxation in polymer nanocomposites near the glass transition. *Macromolecules*, 36, 4010–4016.

- Ma, X. F., Yu, J. G., & Wan, J. J. (2006). Urea and ethanolamine as a mixed plasticizer for thermoplastic starch. *Carbohydrate Polymers*, 64, 267–273.
- Marney, D. C. O., Ruisell, L. J., & Wu, D. Y. (2008). The suitability of halloysites nanotubes as a fire retardant for nylon 6. *Polymer Degradation and Stability*, 93, 1971–1978.
- Mondragón, M., Hernández, E. M., Rivera-Armenta, J. L., & Rodríguez-González, F. J. (2009). Injection molded thermoplastic starch/natural rubber/clay nanocomposites: Morphology and mechanical properties. *Carbohydrate Polymers*, 77, 80–86.
- Nicolini, K. P., Fukamachi, C. R. B., Wypych, F., & Mangrich, A. S. (2009). Dehydrated halloysite intercalated mechanochemically with urea: Thermal behavior and structural aspects. *Journal of Colloid and Interface Science*, 338, 474–479.
- Prashantha, K., Lacrampe, M. F., & Krawczak, P. (2011). Processing and characterization of halloysite nanotubes filled polypropylene nanocomposites based on a masterbatch route: Effect of halloysites treatment on structural and mechanical properties. *Express Polymer Letters*, 5, 295–307.
- Prashantha, K., Schmitt, H., Lacrampe, M. F., & Krawczak, P. (2011). Mechanical behaviour and essential work of fracture of halloysite nanotubes filled polyamide 6 nanocomposites. *Composite Science and Technology*, 71, 1859–1866.
- Shi, R., Liu, Q., Ding, T., Han, Y., Zhang, L., Chen, D., et al. (2007). Ageing of soft thermoplastic starch with high glycerol content. *Polymer Science*, 103, 574–586.
- Soulestin, J., Prashantha, K., Lacrampe, M. F., & Krawczak, P. (2011). Bioplastic based nanocomposites for packaging applications. In P. Srikanth (Ed.), *Handbook of bioplastics and biocomposites engineering applications*, ISBN 978-0470626078 (pp. 77–120). USA: Wiley-Scrivener Publ, 620 p. (Chapter 4).
- Szczygielska, A., & Kijenski, J. (2011). Studies of properties of polypropylene/halloysites composites. *Polish Journal of Chemical Technology*, 13, 61–65.
- Tester, R. F., Karkalasa, J., & Qi, X. (2004). Starch-composition, fine structure and architecture. *Journal of Cereal Science*, 39, 151–165.
- Van Soest, J. J. G., Benes, K., & De Wit, D. (1996). The influence of starch molecular mass on the properties of extruded thermoplastic starch. *Polymer*, 37, 3543–3552.
- Van Soest, J. J. G., De Wit, D., & Vliegthart, J. F. G. (1996). Changes in the mechanical properties of thermoplastic potato starch in relation with changes in B-type crystallinity. *Carbohydrate Polymers*, 29, 225–232.
- Van Soest, J. J. G., Hulleman, S. H. D., De Wit, D., & Vliegthart, J. F. G. (1996). Crystallinity in starch bioplastics. *Industrial Crops and Products*, 5, 11–22.
- Xie, Y., Chang, Y., Wang, S., Yu, J., & Ma, X. (2011). Preparation and properties of halloysite nanotubes/plasticized *Dioscorea opposita* Thunb. starch composites. *Carbohydrate Polymers*, 83, 186–191.
- Yang, B. X., Shi, J. H., Pramoda, K. P., & Goh, S. H. (2007). Enhancement of stiffness, strength, ductility and toughness of poly(ethylene oxide) using phenoxy grafted multi walled carbon nanotubes. *Nanotechnology*, 18, 12, art. no. 125606.
- Yu, L., & Christie, G. (2001). Measurement of starch thermal transitions using differential scanning calorimetry. *Carbohydrate Polymers*, 46, 179–184.
- Zhou, W. Y., Guo, B., Liu, M., Liao, R., Bakr, A., & Jia, D. (2009). Poly(vinyl alcohol)/halloysite nanotubes bionanocomposite films: Properties and in vitro osteoblasts and fibroblasts response. *Journal of Biomedical Materials Research Part A*, 93A, 1574–1587.